Med Chem Res
DOI 10.1007/s00044-016-1520-3

MEDICINAL CHEMISTRY RESEARCH

ORIGINAL RESEARCH

Antidiabetic potential and enzyme kinetics of benzothiazole derivatives and their non-bonded interactions with α-glucosidase and α-amylase

Ninad V. Puranik[1] · Hemalata M. Puntambekar[1] · Pratibha Srivastava[1]

Received: 6 May 2015 / Accepted: 29 January 2016

Abstract Benzothiazole derivatives were synthesized and their antidiabetic potential evaluated using α-glucosidase, α-amylase, non-enzymatic glycosylation of hemoglobin and advanced glycation end product inhibition assays. Compound **3l** showed low IC_{50} values of 0.31, 0.98, 0.59 and 0.19 mM in α-amylase, α-glucosidase, non-enzymatic glycosylation of hemoglobin and AGE inhibition assays, respectively, and outperformed the standard acarbose. Enzyme kinetic studies revealed that it has a K_i of 0.39 and 1.5 mM for α-amylase and α-glucosidase, respectively. The non-bonded interactions of **3l** with α-amylase (3OLD) and α-glucosidase (2ZE0) showed that it binds in the active site pocket and is surrounded by residues Asp197, Glu233, Asp300 in 3OLD and Asp199, Glu256, Asp326 in 2ZE0.

Keywords AGE inhibition · α-Amylase · Benzothiazole derivatives · α-Glucosidase · Non-bonded interactions

Abbreviations

AGE	Advanced glycation end products
AMPK	Adenosine 5′-monophosphate-activated protein kinase
CAZY	Carbohydrate active enzymes database
GH	Glycoside hydrolases
GH31AG	Glycoside hydrolases 31 alpha glucosidase
NIDDM	Non-insulin-dependent diabetes mellitus
PI3Ks	Phosphoinositide 3-kinases
PPHG	Postprandial hyperglycemia
pNPG	*p*-Nitrophenyl glucopyranoside
SBG	Sugar beet glucosidase

✉ Pratibha Srivastava
psrivastava@aripune.org;
psriyns27@gmail.com

[1] Bioprospecting Group, Agharkar Research Institute, G. G. Agarkar Road, Pune, Maharashtra 411004, India

Introduction

Diabetes is a very serious health problem that develops because of insulin resistance or improper function of the pancreas and widely affects millions of people worldwide (Shaw *et al.,* 2010). Diabetes is categorized into two main types, Type I and Type II. The more prevalent, Type II diabetes, or non-insulin-dependent diabetes mellitus (NIDDM), is a metabolic syndrome characterized by a high blood glucose level and generally occurs because of hectic lifestyles and oxidative stress. The treatment of Type II diabetes is quite complex because of the many symptoms associated with the disease, among which elevated postprandial hyperglycemia (PPHG) is a major risk factor (Gin and Rigalleau, 2000). Elevated PPHG is due to the action of glucosidases, a class of enzymes that helps breakdown complex carbohydrates into simple sugars such as maltose and glucose. Glucosidase and α-amylase inhibitors play an important role in controlling elevated PPHG in diabetic patients. These inhibitors slow the action of enzyme, reducing starch hydrolysis and having a beneficial effect on glycemic index management in diabetic patients (Notkins, 2002).

Human pancreatic α-amylase is an enzyme from family 13 of the glycoside hydrolases (GH13[a]), an extremely diverse enzyme family with members that display distinct substrate and product specificities as reflected by the 26

Published online: 19 February 2016

different EC numbers found in this family including: glycoside hydrolases (EC 3.2.1.X, the most abundant), glycoside transferases (EC 2.4.1.X) and even isomerases (EC 5.4.99.15 and EC 5.4.99.16) (Henrissat and Bairoch, 1996; Henrissat *et al.,* 1995; Stam *et al.,* 2006). The α-glucosidase members characterized to date are found in two major families, GH13 and GH31, and two minor families, GH4 and GH97, according to the CAZY classification system (Henrissat and Davies, 1997). They can hydrolyze 1, -4- or 1, -6- bonds of α-D-glucosides at the non-reducing ends with release of α-D-glucose (EC 3.2.1.20) and retention of configuration at the anomeric carbon (Ly and Withers, 1999; McCarter and Withers, 1996).

Although many pharmaceutical treatments for diabetes (Abbatecola *et al.,* 2008) are available, there is still no complete cure for this chronic metabolic disorder. Patients have to tolerate the side effects (Stang *et al.,* 1999) of medication as well as post-diabetic complications such as hypertension, nephrotoxicity and vision problem (Kirk *et al.,* 2005; de Groot *et al.,* 2001; Spiller and Quadrani, 2004). Therefore, there is still a great need for the development of safe and efficacious antidiabetic molecules.

Heterocycles are gold mines in medicinal chemistry. Most drugs used in modern medicine possess a heterocyclic nucleus (Gomtsyan, 2012). One interesting heterocycle is benzothiazole, whose importance in the field of medicinal chemistry is undeniable because of its association with diverse pharmacological activities (Keri *et al.,* 2015). Researchers have reported that benzothiazoles activate the enzyme adenosine 5′-monophosphate-activated protein kinase (AMPK) (Meltzer-Mats *et al.,* 2013), which is involved in the regulation of the glucose transport in skeletal muscle (Fujii *et al.,* 2006) and as an inhibitor of phosphoinositide 3-kinases (PI3Ks, D'Angelo *et al.,* 2011). Medicinal chemists' attention was particularly drawn to this core motif when the clinically available drug riluzole (Miller *et al.,* 2007) was found to act as an anticonvulsant. The diverse nature of this molecule in the field of medicinal chemistry prompted us to evaluate the antidiabetic potential of benzothiazole derivatives. Although there are references in the literature for antidiabetic benzothiazoles (Mariappan *et al.,* 2012; Pattan *et al.,* 2005; Meltzer-Mats *et al.,* 2013), the antidiabetic activity of the benzothiazoles studied in this paper has not previously been explored. Therefore, in this paper, we report the synthesis of benzothiazole derivatives, their effects on enzyme kinetics, and an exploration of their antidiabetic potential using α-amylase, α-glucosidase, non-enzymatic glycosylation and advanced glycation end product (AGE) inhibition assays. A computational study to understand the non-bonded interactions of the molecules with glucosidases from the families GH13 (2ZE0) and GH31 (3W38) and an amylase (3OLD) was carried out.

Experimental section

Materials and methods

α-Amylase was purchased from Himedia, and hemoglobin solution was used as Coral Hemocor D purchased from Coral Clinical System, Goa, India. Glucobay tablets (acarbose tablets) from Bayer Zydus Pharma were used as standard in place of acarbose. Bovine serum albumin, aldehydes and 2-aminothiophenol were used which is obtained from Sigma-Aldrich. α-Glucosidase, *p*-nitrophenyl glucopyranoside (pNPG) and starch were purchased from Sisco Research Laboratory. Glucose, fructose, maltose and organic solvents were purchased from Molychem. ^{1}HNMR and ^{13}CNMR spectra were recorded at room temperature on Varian 400 MHz and Bruker 100 MHz spectrophotometer, respectively. Chemical shift values were reported relative to TMS that was used as an internal standard. The samples were prepared by dissolving the synthesized compounds in DMSO-d_6. Chemical shifts were expressed in δ (ppm) and coupling constants (J) in hertz. The splitting pattern abbreviations are as follows: s, singlet; d, doublet; t, triplet; q, quartet; m, unresolved multiplet due to the field strength of the instrument; dd, doublet of doublet. Column chromatography was performed on Merck silica gel 60 (230–400 mesh; Merck, Darmstadt, Germany). Thin-layer chromatography was carried out on precoated Merck silica gel 60F_{254} (Merck) sheets using UV absorption and iodine physical adsorption for visualization. Discovery studio Visualizer, client version, was used for non-bonded interaction study.

General procedure for the synthesis of 2-substituted benzothiazoles

Synthesis of benzothiazole derivatives(**3 a-p**) was carried out according to the procedure reported by Kenny and Mashelkar (2006). Different benzaldehydes (**2**, 5.5 mmol) and 2-aminothiophenol (**1**, 5 mmol) were taken in a round-bottom flask containing 7 ml of acetic acid. The reaction mixture was refluxed for 5–6 h (Scheme 1). The reaction was monitored by TLC. After completion of the reaction, the reaction mixture was cooled to room temperature and decomposed over ice–water mixture. The solid thus obtained was collected by filtration. The crude product was purified either by crystallization using ethanol or by column chromatography using hexane: ethyl acetate as solvent. All the synthesized compounds were characterized by spectroscopic methods.

*2-(Cyanomethyl)-1,3-benzothiazole (***3a***)* Compound **3a** was obtained as yellowish powder in 75 % yield, Mp 98–100 °C; IR (KBr) ν_{max}: 3061, 2252, 1556, 1433,

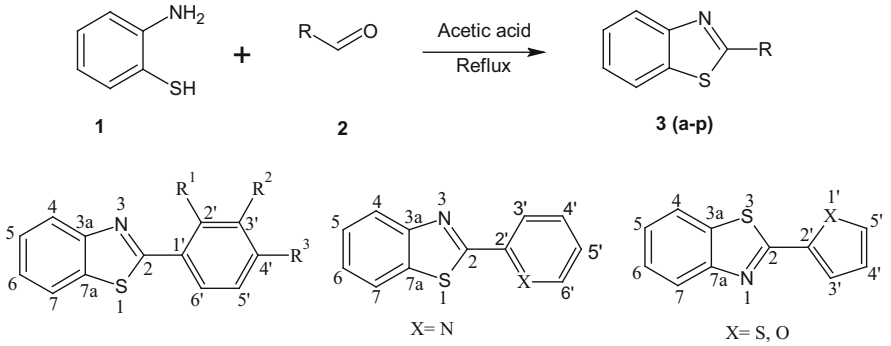

3	a	b	c	d	e	f	g	h	i	j	k	l	m	n	o	p
R	CH_2CN	CH_2Cl	4-$OCH_3C_6H_4$	3-$OCH_3C_6H_4$	3,4- $OCH_3C_6H_3$	4-ClC_6H_4	3,4-ClC_6H_3	4-FC_6H_4	2-OH C_6H_4	4-OH C_6H_4	2,3 -OH C_6H_3	4-(NMe_2) C_6H_4	C_5H_4N	C_4H_3O	C_4H_3S	3-$NO_2C_6H_4$

Scheme 1 Synthesis of benzothiazole derivatives

1307 cm^{-1}; ^1H NMR (DMSO-d_6, 400 MHz): $\delta = 8.2$ (1H, d, $J = 8.0$ Hz, H-7), 8.1 (1H, d, $J = 8.0$, H-4), 7.55 (1H, t, $J = 7.4$ Hz, H-5), 7.45 (1H, t, $J = 7.4$ Hz, H-6), 4.88 (2H, s, CH_2); ^{13}C NMR (DMSO-d_6, 100 MHz): $\delta = 160.4$ (C, C-2), 152.2 (C, C-3a), 135.0 (C, C-7a), 126.4 (CH, C-7), 125.5 (CH, C-6), 122.5 (CH, C-5), 122.2 (CH, C-4), 116.4 (CN, C-2′), 22.3 (CH_2, C-1′); EIMS: m/z 174 [M^+]; Anal. Calcd for $C_9H_6N_2S$: C, 62.04; H, 3.47; N, 16.07 Found: C, 62.11; H, 3.39, N, 16.13.

*2-(Chloromethyl)-1,3-benzothiazole (***3b***)* Compound **3b** was obtained as greenish powder in 58 % yield, Mp 34 °C; IR (KBr) ν_{max}: 3088, 2999, 1514, 1431, 1263, 760 cm^{-1}; ^1H NMR (DMSO-d_6, 400 MHz): $\delta = 7.1$ (1H, d, $J = 7.8$, H-7), 7.0 (1H, d, $J = 7.8$, H-4), 6.7 (1H, t, $J = 7.2$ Hz, H-5), 6.4 (1H, t, $J = 7.2$ Hz, H-6), 5.4 (2H, s, CH_2); ^{13}C NMR (DMSO-d_6, 100 MHz): $\delta = 166.7$ (C, C-2), 152.8 (C, C-3a), 135.8 (C, C-7a), 127.8 (CH, C-7), 125.4 (CH, C-6), 123.4 (CH, C-5), 121.7 (CH, C-4), 42.1 (CH_2, C-1′); EIMS: m/z 183 [M^+] (49), 148 (100), 108 (31.6); Anal. Calcd for C_8H_6ClNS: C, 52.32; H, 3.29; N, 7.62 Found: C, 52.27; H, 3.34; N, 7.56.

*2-(4-Methoxyphenyl)-1,3-benzothiazole (***3c***)* Compound **3c** was obtained as pale yellow powder in 80 % yield, Mp 134 °C; IR (KBr) ν_{max}: 3021, 2835, 1604, 1591, 1485, 833 cm^{-1}; ^1H NMR (DMSO-d_6, 400 MHz): $\delta = 7.95$–8.15 (4H, m, H-4, H-7, H-2′, H-6′), 7.52 (1H, t, $J = 7.6$ Hz, H-5), 7.4 (1H, t, $J = 7.6$ Hz, H-6), 7.1 (2H, d, $J = 8.0$ Hz, H-3′. H-5′), 3.85 (3H, s, OCH_3); ^{13}C NMR (DMSO-d_6, 100 MHz): $\delta = 167.22$ (C, C-2), 161.95 (C, C-4′), 153.87(C, C-3a), 134.43 (C, C-7a), 129.04 (CH, C-6′), 129.04(CH, C-2′), 126.67 (CH, C-5), 125.71 (C, C-1′), 125.25 (CH, C-6), 122.64 (CH, C-4), 122.33 (CH, C-7), 114.9 (CH, C-5′), 114.9 (CH, C-3′), 55.5 (C, –O<u>C</u>H$_3$); EIMS: m/z 243 (12.5), 242 (38), 241 [M^+] (100), 226 (15.8); Anal. Calcd for $C_{14}H_{11}NOS$: C, 69.68; H, 4.59; N, 5.80 Found: C, 69.62; H, 4.64; N, 5.73.

*2-(3-Methoxyphenyl)-1,3-benzothiazole (***3d***)* Compound **3d** was obtained as pale yellow powder in 75 % yield, Mp 120–122 °C; IR (KBr) ν_{max}: 3059, 2962, 2933, 2835, 1604, 1581, 1471, 1431, 987, 761 cm^{-1}; ^1H NMR (DMSO-d_6, 400 MHz): $\delta = 8.18$(1H, d, $J = 8.0$ Hz, H-7), 8.12 (1H, d, $J = 8.0$ Hz, H-4), 7.41–7.71 (5H, m, H-5, H-6, H-2′, H-5′, H-6′), 7.18 (1H, d, $J = 8.0$ Hz, H-4′), 3.9 (3H, s, OCH_3); ^{13}C NMR (DMSO-d_6, 100 MHz): $\delta = 167.8$ (C, C-2), 159.6 (C, C-3′), 153.9 (C, C-3a), 135 (C, C-7a), 134.8 (CH, C-6′), 129.9 (CH, C-2′), 126.2 (CH, C-5), 125.1 (CH, C-6), 123.2 (C, C-1′), 121.5 (CH, C-7), 120.1 (CH, C-4), 117.2 (CH, C-5′), 112.0 (CH, C-4′), 55.5 (C, –O<u>C</u>H$_3$); EIMS: m/z 241 [M^+] (13.73), 211.1 (9.57), 108.1 (22.84); Anal. Calcd for $C_{14}H_{11}NOS$: C, 69.68; H, 4.59; N, 5.80. Found: C, 69.58; H, 4.61, N, 5.71.

*2-(3,4-Dimethoxyphenyl)-1,3-benzothiazole (***3e***)* Compound **3e** was obtained as pink powder in 80 % yield, Mp 132–134 °C; IR (KBr) ν_{max}: 2964, 2939, 2841, 1598, 1521, 1481, 1431, 1338, 808, 763 cm^{-1}; ^1H NMR (DMSO-d_6, 400 MHz): $\delta = 8.10$ (1H, d, $J = 8.0$ Hz, H-7), 8.02 (1H, d, $J = 8.0$ Hz, H-4), 7.60–7.64 (2H, m, H-2′, H-6′), 7.52 (1H, t, $J = 7.4$ Hz, H-5), 7.42(1H, t, $J = 7.4$ Hz, H-6), 7.12 (1H, d, $J = 8.0$ Hz, H-5′), 3.89 (3H, s, OCH_3), 3.85 (3H, s, OCH_3); ^{13}C NMR (DMSO-d_6, 100 MHz): 168.2 (C, C-2), 154.1 (C, C-3a), 151.9 (C, C-3′), 149.6 (C, C-4′),. 134.9 (C, C-7a), 126.7 (C, C-1′), 126.5 (CH, C-5), 125.2 (CH, C-6), 123.0 (CH, C-7), 121.7 (CH, C-4), 121.4 (CH, C-6′), 111.2 (CH,

C-2′), 110.0 (CH, C-5′), 56.4 (C, –O<u>C</u>H$_3$), 56.3 (C, –O<u>C</u>H$_3$); EIMS: 271[M$^+$] (100); Anal. Calcd for $C_{15}H_{13}NO_2S$: C, 66.39; H, 4.82; N, 5.16 Found: C, 66.31; H, 4.88, N, 5.04.

*2-(4-Chlorophenyl)-1,3-benzothiazole (**3f**)* Compound **3f** was obtained as pale yellow powder in 75 % yield, Mp 114–116 °C; IR (KBr) ν_{max}: 3055, 1589, 1435, 1315, 1288, 1089, 966, 756 cm^{-1}; ^{1}H NMR (DMSO-d_6, 400 MHz): $\delta = 8.16$ (1H, d, $J = 8.0$ Hz, H-7), 8.11 (2H, d, $J = 8.0$ Hz, H-3′, H-5′), 8.07 (1H, d, $J = 8.0$ Hz, H-4), 7.64 (2H, d, $J = 8.0$ Hz, H-2′,H-6′), 7.56 (1H, t, $J = 7.4$ Hz, H-5), 7.48 (1H, t, $J = 7.4$ Hz, H-6); ^{13}C NMR (DMSO-d_6, 100 MHz): $\delta = 166.6$ (C, C-2), 154.1 (C, C-3a), 137.0 (C, C-7a), 135.0 (C, C-1′), 132.1 (C, C-4′), 129.3 (CH, C-3′), 129.3 (CH, C-5′), 128.7 (CH, C-2′) 128.7 (CH, C-6′), 126.5 (CH, C-5), 125.4 (CH, C-6), 123.3 (CH, C-4), 121.6 (CH, C-7) EIMS: 245 [M$^+$] (100), 108 (30), 137 (70), 111(13); Anal. Calcd for $C_{13}H_8ClNS$: C, 63.54; H, 3.28; N, 5.70. Found C, 63.62; H, 3.14; N 5.62.

*2-(3,4-Dichlorophenyl)-1,3-benzothiazole (**3g**)* Compound **3g** was obtained as white powder in 90 % yield. Mp 118–119 °C; IR (KBr) ν_{max}: 3062, 1500, 1462, 1433, 1375, 786 cm^{-1}; ^{1}H NMR (DMSO-d_6, 400 MHz): $\delta = 8.3$ (1H, s, H-2′), 8.2 (1H, d, $J = 8.0$ Hz, H-5′), 8.18 (1H, d, $J = 8.0$ Hz, H-6′), 8.1 (1H, d, $J = 8.0$ Hz,H-7), 7.82 (1H, d, $J = 8.0$ Hz, H-4), 7.59 (1H, t, $J = 7.2$ Hz, H-6), 7.42 (1H, t, $J = 7.2$ Hz, H-5); ^{13}C NMR (DMSO-d_6, 100 MHz): $\delta = 164.9$ (C, C-2), 154.6 (C, C-3a), 135.6 (C, C-7a), 135.0 (C, C-4′), 133.9 (C, C-3′), 133.7 (CH, C-2′), 131.0 (CH, C-5′), 129.3 (CH, C-6′), 126.8 (C, C-1′) 126.6 (CH, C-5), 125.8 (CH, C-6), 124, (CH, C-4), 121.8 (CH, C-7). EIMS: 283 (14), 282 (11), 281 (67), 280 [M$^+$] (20), 279 (100); Anal. Calcd for $C_{13}H_7Cl_2NS$: C, 55.73; H, 2.51; N, 4.99. Found: C, 55.61; H, 2.42; N 4.86.

*2-(4-Fluorophenyl)-1,3-benzothiazole (**3h**)* Compound **3h** was obtained as yellowish powder in 82 % yield. Mp 101–103 °C; IR (KBr) ν_{max}: 3057, 1556, 1519, 1350, 1284, 1157, 758, 696 cm^{-1}; ^{1}H NMR (DMSO-d_6, 400 MHz): $\delta = 8.15$–8.18 (3H, m, H-7, H-3′, H-5′), 8.06 (1H, d, $J = 8.0$ Hz, H-4), 7.55 (1H, t, $J = 7.4$ Hz, H-5), 7.48 (2H, d, $J = 8.0$ Hz, H-2′, H-6′), 7.42 (1H, t, $J = 7.4$, H-6); ^{13}C NMR (DMSO-d_6, 100 MHz): $\delta = 163.2$ (C, C-2), 161.3 (C, C-3a), 152.4 (C, C-7a), 142.5 (C, C-1′), 130.3 (C, C-4′), 127.2 (CH, C-3′), 127.2 (CH, C-5′), 124.3 (CH, C-2′), 124.3 (CH, C-6′), 123.8 (CH, C-5), 119.9 (CH, C-6), 117.0 (CH, C-4), 111.4 (CH, C-7); EIMS: 229 [M$^+$] (100); Anal. Calcd for $C_{13}H_8FNS$: C, 68.10; H, 3.51; N 6.11. Found: C, 68.18; H, 3.63; N, 6.03.

*2-(2-Hydroxyphenyl)-1,3-benzothiazole (**3i**)* Compound **3i** was obtained as yellowish powder in 60 % yield, Mp 127–128 °C; IR (KBr) ν_{max}: 3059, 1487, 1438, 1220, 817, 715 cm^{-1}; ^{1}H NMR (DMSO-d_6, 400 MHz): $\delta = 11.6$ (1H, s, OH); 8.17–8.20 (2H, m, H-7, H-6′), 8.08 (1H, d, $J = 8.0$ Hz, H-4), 7.39–7.6 (3H, m, H-4′, H-5′, H-6), 7.1 (1H, d, $J = 8.0$ Hz, H-3′), 7.0 (1H, t, $J = 7.4$ Hz, H-5); ^{13}C NMR (DMSO-d_6, 100 MHz): $\delta = 169.23$ (C, C-2), 157.84, (C, C-3a), 151.68 (C, C-2′), 132.6 (C, C-7a), 132.45 (CH, C-4′), 128.27 (CH, C-6′), 126.52 (CH, C-5), 125.37 (CH, C-6), 122.0 (CH, C-5′), 121.34 (C, C-1′), 119.36 (CH, C-4), 117.73 (CH, C-7) 116.65 (CH, C-3′); EIMS: 227 [M$^+$] (89); Anal. Calcd for $C_{13}H_9NOS$: C, 68.69; H, 3.99; N 6.16. Found: C, 68.58; H, 3.91; N, 6.03.

*2-(4-Hydroxyphenyl)-1,3-benzothiazole (**3j**)* Compound **3j** was obtained as yellowish powder in 70 % yield. Mp 220–224 °C; IR (KBr) ν_{max}: 3053, 2997, 1606, 1454 cm^{-1}; ^{1}H NMR (DMSO-d_6, 400 MHz): $\delta = 10.2$ (1H, s, OH), 8.1 (1H, d, $J = 8.0$ Hz, H-7), 7.9 (3H, dd, $J = 8.0$ Hz, H-4, H-2′, H-6′), 7.5 (1H, t, $J = 7.4$ Hz, H-5), 7.4 (1H, t, $J = 7.4$ Hz, H-6), 6.9 (2H, d, $J = 8.2$ Hz, H-3′, H-5′); 13C NMR (DMSO-d_6, 100 MHz): $\delta = 169.2$ (C, C-2), 160.8 (C, C-4′), 153.8 (C, C-3a), 134.5 (C, C-7a), 129.1 (CH, C-2′), 129.1 (CH, C-6′), 126.3 (CH, C-5), 124.9 (CH, C-6), 124.8 (CH, C-4), 121.9 (C, C-1′), 121.6 (CH, C-7), 115.8 (CH, C-3′) 115.8 (CH, C-5′); EIMS: 227 [M$^+$] (100); Anal. Calcd for $C_{13}H_9NOS$: C, 68.69; H, 3.99; N, 6.16. Found: C, 68.59; H, 3.89; N 6.07.

*2-(2,3-Dihydroxyphenyl)-1,3-benzothiazole (**3k**)* Compound **3k** was obtained as white powder in 75 % yield, Mp 217 °C; IR (KBr) ν_{max}: 3491, 2702, 1601, 1439, 1277, 1182, 905, 756 cm^{-1}; ^{1}H NMR (DMSO-d_6, 400 MHz): $\delta = 11.2$ (1H, broad s, OH), 9.61 (1H, broad s, OH), 8.2 (1H, d, $J = 8.0$ Hz, H-7), 8.05 (1H, d, $J = 8.0$ Hz, H-4), 7.5–7.6 (2H, m, H-6′, H-5), 7.41 (1H, t, $J = 7.4$ Hz, H-6), 6.95 (1H, d, $J = 8.0$ Hz, H-4′), 6.85 (1H, t, $J = 7.4$ Hz, H-5′); ^{13}C NMR (DMSO-d_6, 100 MHz): $\delta = 166.4$ (C, C-2), 151.4 (C, C-3a), 146.3 (C, C-3′), 145.1 (C, C-2′), 133.9 (C, C-7a), 126.6 (CH, C-5), 125.2 (CH, C-6), 122.1 (CH, C-7), 122.0 (CH, C-4), 119.5 (CH, C-5′), 118.5 (CH, C-6′), 118.4 (C, C-1′), 117.7 (CH, C-4′); EIMS: m/z 243 [M$^+$] (79); Anal Calcd for $C_{13}H_9NO_2S$: C, 64.18; H, 3.72; N 5.75. Found: C, 64.08; H, 3.79; N 5.81.

*2-(4′-(N,N-Dimethylamino)phenyl)-1,3-benzothiazole (**3l**)* Compound **3l** was obtained as yellowish powder in 90 % yield, Mp 160–162 °C; IR (KBr) ν_{max}: 3053, 2906, 1610, 1485, 1433, 1371, 1315, 752, 721 cm^{-1}; ^{1}H NMR (DMSO-d_6, 400 MHz): $\delta = 8.05$ (1H, d, $J = 8.0$ Hz, H-7), 7.85–7.95 (3H, m, H-2′, H-6′, H-4), 7.46 (1H, t, $J = 7.4$ Hz, H-5), 7.35 (1H, t, $J = 7.4$ Hz, H-6), 6.8 (2H, d, $J = 8$ Hz, H-3′, H-5′), 3.0 (6H, s, N-CH$_3$); ^{13}C NMR (DMSO-d_6, 100 MHz): $\delta = 168.01$ (C, C-2), 154.09 (C, C-3a), 133.98 (C, C-7a), 128.65, (CH, C-2′), 128.65 (CH, C-6′), 126.47 (CH, C-5), 124.64 (CH, C-6), 122.31 (CH,

C-7), 122.04 (CH, C-4), 120.33 (C, C-1′), 112.0(CH, C-3′), 112.0 (CH, C-5), 39.90 (C, -N<u>C</u>H$_3$), 39.90 (C, -N<u>C</u>H$_3$); EIMS: m/z 256 (4), 255 (15), 254 [M +] (100), 253 (37), 239 (13), 238 (8); Anal Calcd for $C_{15}H_{14}N_2S$: C, 70.83; H, 5.54; N, 11.01; Found: C, 70.88; H, 5.44; N, 11.12.

*2-(Pyridin-2-yl)-1,3-benzothiazole (***3m***)* Compound **3m** was obtained as white powder in 88 % yield. Mp 133–134 °C; IR (KBr) ν_{max}: 3053, 1585, 1566, 1510, 1460, 1433, 1317, 1294, 1265, 783, 721 cm^{-1}; ^{1}H NMR (DMSO-d_6, 400 MHz): $\delta = 8.7$ (1H, d, $J = 8.0$ Hz, H-6′), 8.35 (1H, d, $J = 8.0$ Hz, H-3′), 8.2 (1H, d, $J = 8.0$ Hz, H-7), 8.1 (1H, d, $J = 8.0$ Hz, H-4), 8.05 (1H, t, $J = 7.4$ Hz, H-4′), 7.55–7.61 (2H, m, H-6, H-5′), 7.5 (1H, t, $J = 7.2$ Hz, H-5); ^{13}C NMR (DMSO-d_6, 100 MHz): $\delta = 169.50$ (C, C-2), 154.21 (C, C-3a), 150.78 (C, C-2′), 150.44 (CH, C-6′), 138.37 (CH, C-4′), 135.86 (C, C-7a), 127.11 (CH, C-5), 126.64 (CH, C-3′), 126.45 (CH, C-6), 123.76 (CH, C-4), 123.05 (CH, C-7), 120.82 (CH, C-5′); EIMS: m/z 213 [M^{+1}] (80); Anal Calcd for $C_{12}H_8N_2S$: C, 67.89; H, 3.79; N, 13.19. Found: C, 68.00; H, 3.85; N13.15.

*2-(Furan-2-yl)-1,3-benzothiazole (***3n***)* Compound **3n** was obtained as yellowish powder in 70 % yield, Mp 102–104 °C; IR (KBr) ν_{max}: 3051, 2956, 1732, 1579, 1246, 1012, 896, 746 cm^{-1}; ^{1}H NMR (DMSO-d_6, 400 MHz): $\delta = 8.14$ (1H, d, $J = 8.0$ Hz, H-7), 8.02 (2H, d, $J = 8.0$ Hz, H-4, H-5′), 7.52 (1H, t, $J = 7.4$ Hz, H-5), 7.47 (1H, t, $J = 7.4$ Hz, H-6), 7.36 (1H, d, $J = 5.2$ Hz, H-3′), 6.78–6.80 (1H, m, H-4′); ^{13}C NMR (DMSO-d_6, 100 MHz): $\delta = 157.30$ (C, C-2), 153.79 (C, C-3a), 148.39 (C, C-2′), 146.65 (CH, C-5′), 134.12 (C, C-7a), 127.27 (CH, C-3′), 125.92 (CH, C-4′), 123.13 (CH, C-5), 122.88 (CH, C-6), 113.57 (CH, C-4), 112.41 (CH, C-7); EIMS: m/z 201[M$^+$] (64); Anal Calcd for $C_{11}H_7NOS$: C, 65.65; H, 3.50; N, 6.96. Found: C, 65.58; H, 3.59; N, 6.90.

*2-(Thiophen-2-yl)-1,3-benzothiazole (***3o***)* Compound **3o** was obtained as pale yellow powder in 85 % yield. Mp 181–183 °C; IR (KBr) ν_{max}: 3057, 1591, 1247, 1010, 746, cm^{-1}; ^{1}H NMR (DMSO-d_6, 400 MHz): $\delta = 8.10$ (1H, d, $J = 8.0$ Hz, H-7), 7.99 (1H, d, $J = 8.0$ Hz, H-4), 7.84–7.87 (2H, m, H-3′, H-5′), 7.52 (1H, t, $J = 7.4$ Hz, H-5), 7.44 (1H, t, $J = 7.4$ Hz, H-6), 7.24 (1H, t, $J = 4.8$ Hz, H-4′); ^{13}C NMR (DMSO-d_6, 100 MHz): $\delta = 161.35$ (C, C-2), 153.65 (C, C-3a), 137.30 (C, C-2′), 134.65 (C, C-7a), 129.27 (CH, C-5′), 128.58 (CH, C-3′), 128.01 (CH, C-4′), 126.40 (CH, C-5), 125.19 (CH, C-6), 122.94 (CH, C-4), 121.42 (CH, C-7); EIMS: m/z 218 [M^{+1}] (79) Anal Calcd for $C_{11}H_7NS_2$: C, 60.79; H, 3.24; N, 6.44 Found: C, 60.71; H,3.18; N, 6.34.

*2-(3-Nitrophenyl)-1,3-benzothiazole (***3p***)* Compound **3p** was obtained as pale yellow powder in 60 % yield. Mp 94–96 °C; IR (KBr) ν_{max}: 3402, 2937, 1529, 1461, 1347, 1107, 1048, 731 cm^{-1}; ^{1}H NMR (DMSO-d_6, 400 MHz): $\delta = 8.51$ (1H, d, $J = 8.0$ Hz, H-4′), 8.41 (1H, d, $J = 8.0$ Hz, H-6′), 8.37 (1H, s, H-2′), 8.23 (1H, d, $J = 8.0$ Hz, H-7), 8.15 (1H, d, $J = 8.0$ Hz, H-4), 7.88 (1H, t, $J = 8.0$ Hz, H-5′), 7.61 (1H, t, $J = 7.4$ Hz, H-5),7.53 (1H, t, $J = 7.4$ Hz, H-6); ^{13}C NMR (DMSO-d_6, 100 MHz): $\delta = 164.9$ (C, C-2), 154.0 (C, C-3a), 148.8 (C, C-1′), 135.4 (C, C-7a), 135.3 (C, C-3), 135.3 (C, C-3′), 133.1 (CH, C-2′), 130.2 (CH, C-6′), 126.9 (CH, C-4′), 126.1 (CH, C-5′), 125.2 (CH, C-5), 123.8 (CH, C-6), 122.4 (CH, C-4), 121.9 (CH, C-7); EIMS: m/z 256 [M$^+$] (65); Anal Calcd for $C_{13}H_8N_2O_2S$: C, 60.92; H, 3.14; N, 10.93. Found: C, 60.75; H, 3.22; N, 10.89.

α-Glucosidase inhibition assay

The inhibitory potential of benzothiazole derivatives on α-glucosidase was determined by glucosidase inhibition assay reported by Dong *et al.* (2012). In brief, 30 µl of test sample (50–1500 µg/ml in methanol) was incubated with 60 µl of α-glucosidase (1 U/ml) for 15 min at 37 °C. After preincubation, 60 µl *p*-nitrophenyl-α-D-glucopyranoside (pNPG, 5 mM, in 10 mM Sodium phosphate buffer, pH 6.8) was added and further incubated for 15 min at 37 °C. The reaction was then stopped by addition of 240 µl of 20 mM Na_2CO_3. The absorbance was monitored at 405 nm. Blank was without the enzyme, and control was without the test sample. Acarbose (Glucobay tablet) was used as a standard. The α-glucosidase inhibitory potential was expressed as inhibition % and calculated as per the formula: % inhibition = (Ac − At)/Ac × 100, where Ac is the absorbance of control and At is the absorbance of the test sample. The concentration of benzothiazole derivative required for inhibiting 50 % of the α-glucosidase activity was defined as IC_{50} value.

α-Amylase inhibition assay

Determination of α-amylase inhibition was carried out as per the protocol reported by Fuwa (1954) with slight modifications. The mixture containing test sample of different concentrations in methanol (200 µl, 50–1000 µg/ml), potato starch, (200 µl, 1 % w/v in 10 mM acetate buffer), α-amylase (200 µl, 1 % w/v in 10 mM acetate buffer) and 400 µl of 10 mM acetate buffer was incubated for 1 h at 37 °C. Then, 20 µl of iodine reagent (0.2 % iodine and 0.2 % potassium iodide) was added to the reaction mixture. Absorbance was observed at 565 nm. Blank was prepared without the enzyme, and control was prepared without the test sample. Acarbose (Glucobay tablet) was used as a standard. The α-amylase inhibitory potential was expressed as % inhibition and calculated as

per the formula: % inhibition = (At − Ac)/At × 100, where Ac is the absorbance of control and At is the absorbance of the test sample. The concentration of benzothiazole derivative required for inhibiting 50 % of the α-amylase activity was defined as IC_{50} value.

Kinetics of α-amylase inhibition

The substrate for amylase is starch. Kinetics of α-amylase with increasing concentration of starch was carried out, and Michaelis–Menten constant (K_m) and maximum velocity (V_{max}) were derived. The kinetics of inhibition of α-amylase by the benzothiazole derivatives was conducted with IC_{50} concentrations, according to the reported procedure (Kazeem *et al.,* 2013). Briefly, 200 µl of the test sample was incubated with 200 µl of α-amylase (1 % w/v in 10 mM acetate buffer), increasing concentration of potato starch (200 µl, 50 µg-5 mg/ml in 10 mM acetate buffer), and 400 µl of 10 mM acetate buffer for 1 h at 37 °C. Then, 20 µl of iodine reagent (0.2 % iodine and 0.2 % potassium iodide) was added to the reaction mixture. The amount of starch remained unused was determined by taking the absorbance at 565 nm and converted to reaction velocity (V_i). Michaelis–Menten plot and Lineweaver–Burk plot (double reciprocal plot) were plotted between substrate concentration (**S**) *verses* reaction velocity (V_i) and $1/V_i$ verses $1/S$, respectively, to determine K_i and $V_{max.}$

Kinetics of α-glucosidase inhibition

The substrate for α-glucosidase is *p*-nitrophenyl-α-D-glucopyranoside. Kinetics of α-glucosidase (30 µl of 1 U/ml) with increasing concentration of *p*-nitrophenyl-α-D-glucopyranoside (250 µg–5 mg/ml) was carried out, and Michaelis–Menten constant affinity (K_m) and maximum velocity (V_{max}) were derived. The kinetics of inhibition of α-glucosidase by the benzothiazole derivatives was conducted with lowest IC_{50} concentration according to the reported procedure (Kazeem *et al.,* 2013). In brief, 30 µl of test sample (100–500 µg/ml in methanol) was incubated with 60 µl of α-glucosidase (1 U/ml) for 15 min at 37 °C. After preincubation, 60 µl *p*-nitrophenyl-α-D-glucopyranoside (pNPG, 250 µg–5 mg/ml, in 10 mM sodium phosphate buffer, pH 6.8) was added and further incubated for 15 min at 37 °C. The reaction was then stopped by addition of 240 µl of 20 mM Na_2CO_3. The amount of p-nitrophenol produced was determined by taking the absorbance at 405 nm and converted to reaction velocity (V_i). Michaelis–Menten plot and Lineweaver–Burk plot (double reciprocal plot) were plotted between substrate concentration (**S**) *verses* reaction velocity (V_i) and $1/V_i$ *verses* 1/S, respectively, to determine K_i and $V_{max.}$

In vitro non-enzymatic glycosylation of hemoglobin

Non-enzymatic glycosylation of hemoglobin is an indicator of diabetic control. We followed the reported procedure by Gragnoli *et al.,* (1982). Glucose (2 %), hemoglobin (0.06 %) and gentamycin (0.02 %) solutions were prepared in phosphate buffer (0.01 M, pH 7.4). Hundred microliters of each solution was mixed with 100 µl different concentration of benzothiazole derivatives. Mixture was incubated in dark for 72 h. The absorbance was monitored at 520 nm. The % inhibition was calculated as per the formula: % inhibition = (At − Ac)/At × 100, where Ac is the absorbance of the control and At is the absorbance of the test sample. Control was prepared without the test sample. Acarbose was used as a standard. The concentration of benzothiazole derivative required for inhibiting 50 % of the hemoglobin glycosylation was defined as IC_{50} value.

Assay for inhibitory activity of AGE formation

The inhibitory activity of AGE formation was measured as per the protocol reported by Jung *et al.* (2013). The AGE reaction solution was prepared by mixing 10 mg/ml bovine serum albumin in 50 mM sodium phosphate buffer (pH 7.4), with 0.02 % sodium azide (added to prevent bacterial growth), 0.2 M fructose and 0.2 M glucose. Test solution of different concentrations (50 µl, 50–500 µg/ml) was added to 950 µl of the AGE reaction solution. The reaction mixture was incubated at 37 °C for 7 days. The fluorescence intensity of the reaction products was measured using a spectrofluorometric detector at excitation and emission wavelengths of 350 and 450 nm, respectively. Phloroglucinol was used as a reference. The mixture without test sample was used as a control. The % inhibition of AGE formation was calculated as per the formula: % Inhibition = [1 − fluorescence of the test sample/fluorescence of the control sample] × 100. 50 % inhibition was measured as IC_{50} value.

Molecular modeling: non-bonded interactions

The non-bonded interaction study was carried out using a Discovery Studio Visualizer 4.0, client version. The PDB file of the α-glucosidase from GH31 family (PDB code 3W38) isolated from sugar beet and GH13 family (PDB code 2ZE0) isolated from deepest sea bacteria was downloaded from www.rcsb.org. The PDB file of α-amylase (PDB code 3OLD) of human pancreatic amylase was also downloaded from the same site. The PDB files of small organic molecules were prepared using Argus software. The homology of α-glucosidase from both the family has been carried out using the sequence alignment

Table 1 Antidiabetic activity and enzyme kinetics of benzothiazole derivatives

No.	IC_{50} α-amylase inhibition (mM)	IC_{50} α-glucosidase (mM)	Non-enzymatic glycosylation (mM)	AGE inhibition (mM)	K_i (α-amylase)	K_i (α-glucosidase)
3a.	Inactive	Inactive	Inactive	Inactive	–	–
3b.	4.91	2.73	3.82	Inactive	–	–
3c.	0.82	1.03	1.03	Inactive	0.62	1.86
3d.	2.07	1.03	2.07	Inactive	0.41	1.86
3e.	Inactive	Inactive	Inactive	Inactive	–	–
3f.	0.61	2.04	2.04	0.40	0.40	–
3g.	0.35	0.89	0.89	0.71	0.35	1.6
3h.	2.62	2.18	3.49	1.74	0.65	1.96
3i.	1.1	6.6	1.76	0.22	–	–
3j.	Inactive	Inactive	Inactive	Inactive	–	–
3k.	0.51	2.05	1.02	Inactive	–	–
3l.	0.31	0.98	0.59	0.19	0.39	1.57
3m	Inactive	Inactive	Inactive	Inactive	–	–
3n.	Inactive	Inactive	Inactive	Inactive	–	–
3o.	Inactive	Inactive	Inactive	Inactive	–	–
3p.	Inactive	Inactive	Inactive	Inactive	–	–
Std[1]	1.16	1.54		1.54		
Std[2]	–	–	3.14			

Std[1] is acarbose (Glucobay tablets) while Std[2] is phloroglucinol

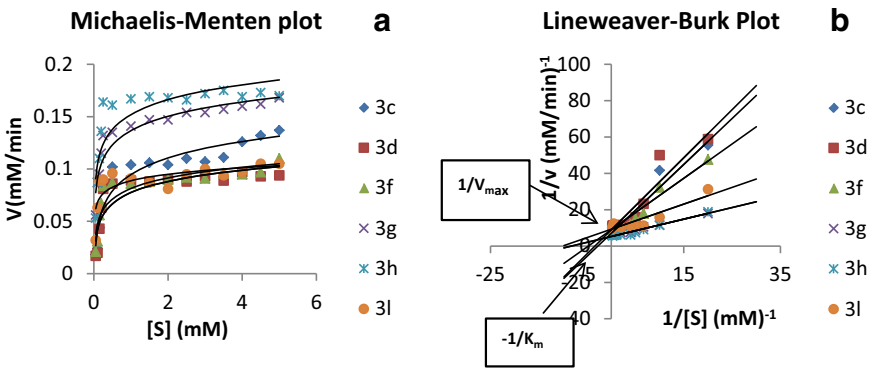

Fig. 1 Enzyme kinetics of α-amylase

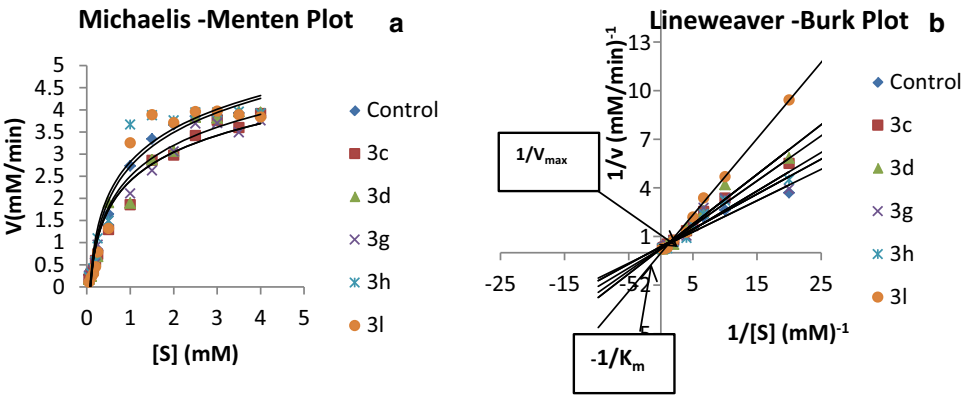

Fig. 2 Enzyme kinetics of α-glucosidase

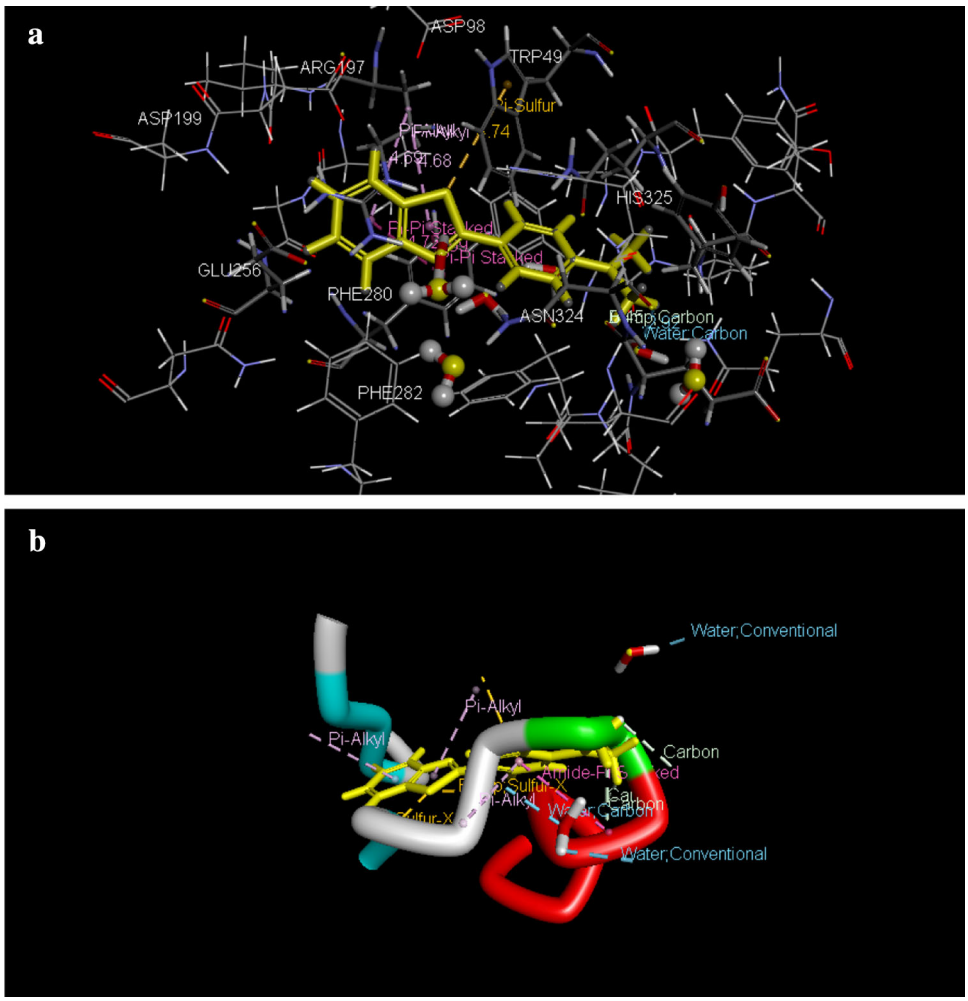

Fig. 3 **a** Non-bonded interaction of **3l** with α-glucosidase 2ZE0 from G13 family. **b** Non-bonded interaction of **3l** with α-glucosidase 2ZE0 from G13 family

option of DSV. The non-bonded interactions were carried out using DSV under the option receptor–ligand interaction. Favorable interactions were hydrogen bond, electrostatic and hydrophobic. The CHARMm force field was applied.

Results and discussion

Chemistry

The diabetes control and complication trial were conducted for 9 years on 1441 patients; it was found that regulation of blood glucose level is an important factor to prevent long-term complications associated with diabetes such as nephropathy, neuropathy and retinopathy (Creutzfeldt, 1999). Glycated hemoglobin is an end product of the glycation process and is an indicator of prolonged hyperglycemia in diabetic patients. The α-glucosidase inhibitor acarbose reduces blood glucose and HbA1C levels in patients with Type II diabetes. This was demonstrated by acarbose monotherapy and treatment with acarbose in combination with oral antidiabetic drugs or insulin (Hoffman and Spengler, 1994; Josse, 1995; Chiasson *et al.*, 1994). To evaluate whether the novel benzothiazole derivatives (Scheme 1) possess useful bioactivity, α-amylase, α-glucosidase, non-enzymatic glycosylation and AGE inhibition assays were carried out. The results indicated that Compound **3l** showed good activity with IC_{50} values of 0.31, 0.98, 0.59 and 0.19 mM for α-amylase, α-glucosidase, non-enzymatic glycosylation and AGE inhibition assays, respectively. Compounds **3f**, **3g** and **3h** also showed activity in all the assays; however, **3h** showed activity at higher concentrations than did **3f** and **3g**, possibly because of the highly electronegative nature of the fluorine substituent.

The compound with a nitro substituent at position 2 of benzothiazole (**3p**) was completely unable to inhibit any of the enzymes. Compounds **3c** and **3d** with methoxy substituents at different positions on the phenyl ring

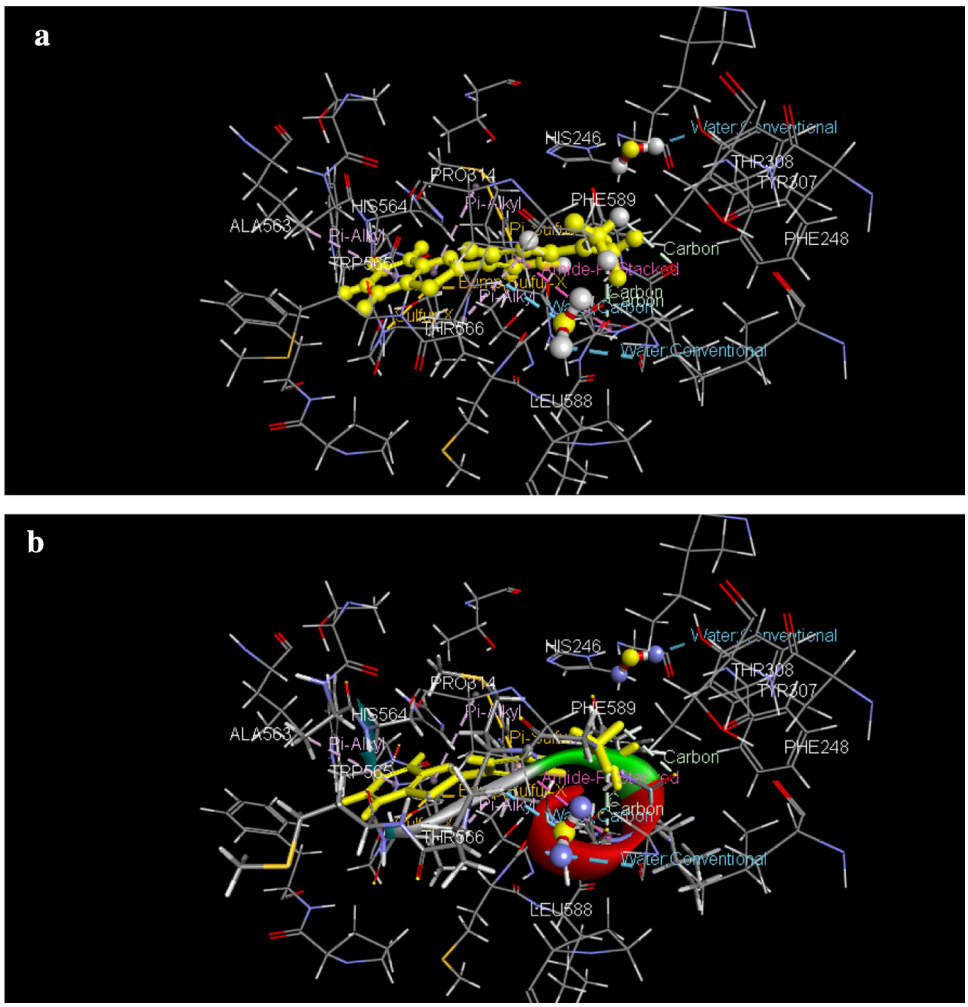

Fig. 4 **a** Non-bonded interaction of **3l** with α-glucosidase 3W38 from G31 family. **b** Non-bonded interaction of **3l** with α-glucosidase 3W38 from G31 family

showed inhibition of α-amylase, α-glucosidase and non-enzymatic glycosylation but could not effectively inhibit AGE. However, the compound **3e** with methoxy substituents at positions 3 and 4 of the phenyl ring was unable to inhibit any of the enzymes, probably because of the high hydrophobicity of the molecule as well as likely steric hindrance. We tested the activity of compounds with an aliphatic substituent at position 2 (**3a** and **3b**); the cyanomethyl derivative (**3a**) was found to be totally inactive, whereas the chloromethyl (**3b**) derivative was active at higher concentrations. A compound with a hydroxyl substituent at the ortho position of the phenyl ring (**3i**) was able to inhibit α-glucosidase, but only at high concentrations. The compound **3j** was totally ineffective. Compound **3h**, with a fluoro substituent, showed activity at higher concentrations, whereas compound **3p** with a nitro substituent was totally inactive. These results indicated that more electronegative substituents reduced the activity. The benzothiazole derivatives with nitro, hydroxyl and dimethoxy substituents are completely inactive, whereas the compounds with *N*,*N*-dimethylamino, chloro, methoxy and dihydroxy substituents showed good activity. This indicated that there must be some correlation in the structure activity relationship of these compounds. It can be interpreted from the findings that benzothiazole derivatives not only inhibit α-glucosidase and α-amylase, but they are capable of inhibiting hemoglobin acylation as well as advanced glycation, which is the end product formed in prolonged diabetes. A comprehensive list of all the compounds studied and their activities are presented in Table 1.

Enzyme kinetics

The K_i of all the active molecules are given in Table 1. Amylase uses starch as a substrate, and unconsumed starch remaining at the end of an amylase digestion was detected by the reaction with iodine form a blue color complex. In the control, when there is no inhibitor, almost all the starch is digested so no color was seen when iodine was added. In

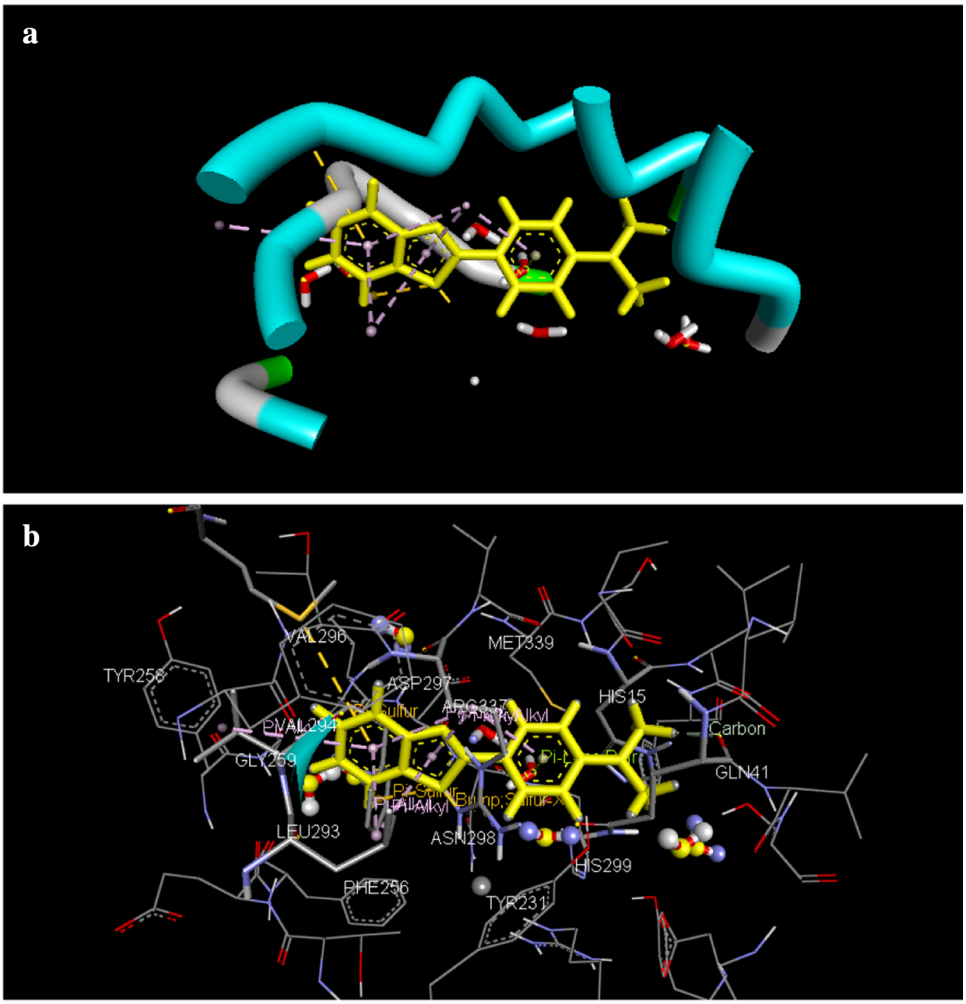

Fig. 5 **a** Non-bonded interaction of **3l** with α-amylase 3OLD. **b** Non-bonded interaction of **3l** with α-amylase 3OLD

the presence of an inhibitor, amylase could no longer digest all of the starch substrate so on iodine addition we observed formation of the blue complex. At high substrate concentrations, amylase was able to approach V_{max} in the presence of benzothiazole derivatives, indicating that these inhibitors are competitive. In the absence of inhibitor, glucosidase hydrolyzes the substrate *p*-NPG and releases *p*-nitrophenol, which gives an intense yellow color. The benzothiazoles showed non-competitive inhibition, as they gave almost the same hyperbolic distribution as the control. Data are presented in Table 1. The kinetic graphs for α-amylase and α-glucosidase are presented in Figs. 1a, b and 2a, b, respectively.

Non-bonded interactions

Non-bonded interactions that form between two partner molecules are the basis of molecular recognition in biological systems. A detailed and comprehensive understanding of non-bonded interactions is crucial in structure-based design, in which identifying and optimizing the molecular interactions between ligands and their host receptor are a fundamental process. According to the crystal structure solved by Shirai *et al.* (2008) to 2.0 Å (2ZE0), α-glucosidase consists of three domains. The N-terminal domain (residues 2–102, 170–205 and 229–471) has a $(\beta/\alpha)_8$-barrel fold and harbors the catalytic center. The subdomain (residues 103–169 and 206–228) is inserted into the N-terminal domain. The C-terminal domain is a β-sandwich fold (residues 472–551). The highly conserved catalytic residues in the GH13 family are Asp199, Glu256, Asp326 in GSJ (α-glucosidase), and the residues important for substrate binding are Tyr63, His103 and His325. The benzothiazole derivative 2-(4'-(*N*,*N*-Dimethylamino)phenyl)-1,3-benzothiazole (**3l**) is closely surrounded by these residues as depicted in Fig. 3a, b. It shows a π-sulfur interaction with Trp49 and a π–π interaction with Arg197, and distances of these bonds were 4.69 and 4.68 Å, respectively. It has also formed a π–π stacking interaction with Phe280 with a bond distance of 3.69 Å. The presence of the benzothiazole

molecule in the active site pocket indicates its selective recognition by α-glucosidase.

The interaction of **3l** with α-glucosidase from GH31 family is shown in Fig. 4a, b. The crystal structure of 3W38 by Tagami *et al.,* (2013) revealed that the major domain of GH31AGs displays a $(\beta/\alpha)_8$-barrel fold. The active site pocket is formed by the $(\beta/\alpha)_8$ and the N-loop in the GH13 family. The overall structure of the SBG 3W38 was divided into four major domains and two subdomains similar to the other GH31AGs: the N-terminal β-sandwich domain (residues 39–298), the $(\beta/\alpha)_8$-barrel domain (residues 229–670), the insertion subdomain b1 (residues 399–443) and b2 (residues 474–519), the proximal C-terminal domain (residues 671–756) and the distal C-terminal domain (residues 757–909). The active site pocket of the 3W38 is formed mainly by the $(\beta/\alpha)_8$ barrel domain and is extended by the N-loop. The molecule **3l** shows a π-alkyl interaction with Ala563. Figure 4a, b illustrates that *N*,*N*-dimethylamino group of **3l** is surrounded by the Asn585-Gly590 loop. Met591 also shows a π-alkyl interaction with the benzothiazole moiety.

A sequence alignment of 2ZE0 and 3W38 showed that they share a sequence identity of 6.2 % and sequence similarity of 19.4 %. Therefore, there was a difference between the binding modes of benzothiazole **3l** with 2ZE0 and 3W38.

The structure of human pancreatic amylase at 1.8 Å was reported by Brayer *et al.* (1995) and revealed that amylase is composed of three structural domains. The largest domain A (residues 1–99 and 169–404) forms a central eight-stranded parallel β-barrel, to one end of which are located the active site residues Asp197, Glu233 and Asp300. Furthermore, a chloride ion is bound in this vicinity and forms ligand interactions to Arg195, Asn298, and Arg337. Domain B is the smallest (residues 100–168) and serves to form a calcium binding site against the wall of the β-barrel of domain A. Domain C (residues 405–496) has an antiparallel β-structure and is loosely associated with domains A and B. The benzothiazole derivative (**3l**) is surrounded very closely by Arg195, Asn298 and Arg337, highlighting its interaction with the residues of the active site pocket (Fig. 5a, b). Figure 5a, b also shows its π-interaction with Val294, Val296, and Leu293. The residues Leu292 to Asn298 form a pocket around the benzothiazole molecule. From this study, it is clear that the molecule **3l** interacts with the core of the enzyme and binds very closely to the active site.

Conclusion

Various substituted benzothiazole derivatives were synthesized and tested for their antidiabetic potential using α-glucosidase, α-amylase, non-enzymatic glycosylation of hemoglobin and advanced glycation end product formation (AGE) inhibition assays. Among the tested benzothiazole derivatives, the compound 2-(4'-(*N*,*N*-Dimethylamino) phenyl)-1,3-benzothiazole (**3l**) was found to be the most active in all the assays. Compound **3l** formed non-bonded interactions with α-glucosidase and α-amylase enzymes. In view of these findings, three pharmacophoric features were found to be important for biological activity (hydrophobic, aromatic and hydrogen bonded interactions). Given these encouraging results, there is still scope to study further benzothiazole derivatives and identify molecules with improved activity against these important enzyme targets.

Acknowledgments Authors are thankful to Agharkar Research Institute for providing financial support as well as for infrastructure. We are also thankful to Ms. Manisha Kharade for helping us to download client version of Discovery Studio Visualizer.

References

Abbatecola AM, Maggi S, Paolisso G (2008) New approaches to treating type 2 diabetes mellitus in the elderly: role of incretin therapies. Drug Aging 25:913–925

Brayer GD, Luo Y, Withers SG (1995) The structure of human pancreatic α-amylase at 1.8 Å resolution and comparisons with related enzymes. Protein Sci 4:1730–1742

Chiasson JL, Josse RG, Hunt JA, Palmason C, Rodger NW, Ross SA, Ryan EA, Tan MH, Wolever TM (1994) The efficacy of acarbose in the treatment of patients with non-insulin dependent diabetes mellitus. Ann Intern Med 121:928–935

Creutzfeldt W (1999) Effects of the α-glucosidase inhibitor acarbose on the development of long-term complications in diabetic animals: pathophysiological and therapeutic implications. Diabetes Metab Res Rev 15:289–296

D'Angelo ND, Kim TS, Andrews K, Booker SK, Caenepeel S, Chen K, D'Amico D, Freeman D, Jiang J, Liu L, McCarter JD, SanMiguel TS, Mullady EL, Schrag M, Subramanian R, Tang J, Wahl RC, Wang L, Whittington DA, Wu T, Xi N, Xu Y, Yakowec P, Yang K, Zalameda LP, Zhang N, Hughes P, Norman MH (2011) Discovery and optimization of a series of benzothiazole phosphoinositide 3-kinase (PI3K)/mammalian target of rapamycin (mTOR) dual inhibitors. J Med Chem 54:1789–1811

de Groot M, Anderson R, Freedland KE, Clouse RE, Lustman PJ (2001) Association of depression and diabetes complications: a meta-analysis. Psychosom Med 63:619–630

Dong HQ, Li M, Zhu F, Liu FL, Huang JB (2012) The inhibitory potential of trilobatin from *Lithocarpus polystachyus* Rehd against α-glucosidase and α-amylase linked to type 2 diabetes. Food Chem 130:261–266

Fujii N, Jessen N, Goodyear LJ (2006) AMP-activated protein kinase and the regulation of glucose transport. Am J Physiol Endocrinol Metab 291:E867–E877

Fuwa H (1954) A new method of micro determination of amylase activity by the use of amylose as the substrate. J Biochem 41:583–603

Gin H, Rigalleau V (2000) Post-prandial hyperglycemia. Post-prandial hyperglycemia and diabetes. Diabetes Metab 26:265–272

Gomtsyan A (2012) Heterocycles in drugs and drug discovery. Chem Heterocycl Compd 48:7–10

Gragnoli G, Tanganelli I, Signorini AM, Tarli P, Paoli C (1982) Non-enzymatic glycosylation of serum proteins as an indicator of diabetic control. Acta Diabetol Lat 19:161–166

Henrissat B, Bairoch A (1996) Updating the sequence-based classification of glycosyl hydrolases. Biochem J 316:695–696

Henrissat B, Davies G (1997) Structural and sequence-based classification of glycoside hydrolases. Curr Opin Struct Biol 7:637–644

Henrissat B, Callebaut I, Fabrega S, Lehn P, Mornon JP, Davies G (1995) Conserved catalytic machinery and the prediction of a common fold for several families of glycosyl hydrolases. Proc Natl Acad Sci USA 92:7090–7094

Hoffman J, Spengler M (1994) Efficacy of 24-week monotherapy with acarbose, glibenclamide or placebo in NIDDM patients. The Essen study. Diabetes Care 17:561–566

Josse RG (1995) Acarbose for the treatment of Type II diabetes: the results of a Canadian multi-centre trial. Diabetes Res Clin Pract 28:S167–S172

Jung HA, Islam MN, Lee CM, Oh SH, Lee S, Jung JH, Choi JS (2013) Kinetics and molecular docking studies of an anti-diabetic complication inhibitor fucosterol from edible brown algae *Eisenia bicyclis* and *Ecklonia stolonifera*. Chem Biol Interact 206:55–62

Kazeem MI, Adamson JO, Ogunwande IA (2013) Modes of inhibition of α-amylase and α-glucosidase by aqueous extract of *Morinda lucida* benth leaf. Biomed Res Int 2013:1–6

Kenny RS, Mashelkar UC (2006) Synthesis of 2- aryl and coumarin substituted benzothiazole derivatives. J Heterocycl Chem 43:1367–1369

Keri RS, Patil MR, Patil SA, Budagumpi S (2015) A comprehensive review in current developments of benzothiazole based molecules in medicinal chemistry. Eur J Med Chem 89:207–251

Kirk JK, Bell RA, Bertoni AG, Arcury TA, Quandt SA, Goff DC (2005) Ethnic disparities control of glycemia, blood pressure and LDL cholesterol among US adults with type 2 diabetes. Ann Phamacother 39:1489–1501

Ly HD, Withers SG (1999) Mutagenesis of glycosidases. Annu Rev Biochem 68:487–522

Mariappan G, Prabhat P, Sutharson L, Banerjee J, Patangia U, Nath S (2012) Synthesis and antidiabetic evaluation of benzothiazole derivatives. J Kor Chem Soc 56:251–256

McCarter JD, Withers SG (1996) Unequivocal identification of Asp-214 as the catalytic nucleophile of *Saccharomyces cerevisiae* a-glucosidase using 5-fluoro glycosyl fluoride. J Biol Chem 271:6889–6894

Meltzer-Mats E, Babai-Shani G, Pasternak L, Uritsky N, Getter T, Viskind O, Eckel J, Cerasi E, Senderowitz H, Sasson S, Gruzman A (2013) Synthesis and mechanism of hypoglycemic activity of benzothiazole derivatives. J Med Chem 56:5335–5350

Miller RG, Mitchell JD, Lyon M, Moore DH (2007) Riluzole for amyotrophic lateral sclerosis (ALS)/motor neuron disease (MND). Cochrane Database Syst Rev 1–29. doi:10.1002/14651858.CD001447.pub2

Notkins AL (2002) Immunologic and genetic factors in type 1 diabetes. J Biol Chem 277:43545–43548

Pattan SR, Suresh C, Pujar VD, Reddy VVK, Pascal VP, Kotti VC (2005) Synthesis and antidiabetic activity of 2-amino[5′(4-sulphonylbenzylidene)-2,4-thiazolidinedione]-7-chloro-6-fluorobenzothiazole. Ind J Chem B 44:2404–2408

Shaw JE, Sicree RA, Zimmet PZ (2010) Global estimates of the prevalence of diabetes for 2010 and 2030. Diabetes Res Clin Pract 87:4–14

Shirai T, Hung VS, Morinaka K, Kobayashi T, Ito S (2008) Crystal structure of GH13 α-glucosidase GSJ from one of the deepest sea bacteria. Proteins 73:126–133

Spiller HA, Quadrani DA (2004) Toxic effects from metformin exposure. Ann Pharmacother 38:776–780

Stam MR, Danchin EGJ, Rancurel C, Coutinho PM, Henrissat B (2006) Dividing the large glycoside hydrolase family 13 into subfamilies: towards improved functional annotations of α-amylase-related proteins. Protein Eng Des Sel 19:555–562

Stang M, Wysowski DK, Butler-Jones D (1999) Incidence of lactic acidosis in metformin user. Diabetes Care 22:925–927

Tagami T, Yamashita K, Okuyama M, Mori H, Yao M, Kimura A (2013) Molecular basis for the recognition of long-chain substrates by plant α-glucosidases. J Biol Chem 288:19296–19303